JCTC Journal of Chemical Theory and Computation

Letter

pubs.acs.org/JCTC

Ionic Liquids Can Selectively Change the Conformational Free-Energy Landscape of Sugar Rings

Zack Jarin and Jim Pfaendtner*

Department of Chemical Engineering, University of Washington, Seattle, Washington, United States

Supporting Information

ABSTRACT: We investigated the conformational free energy landscape of glucose solvated in water and in the ionic liquids (ILs) 1-butyl-3-methylimidazolium chloride ([Bmim][Cl]) and 1-butyl-3-methylimidazoulim boron tetrafluoride ([Bmim][BF_4]). To quantify equilibrium thermodynamic solvent effects, molecular dynamics simulations in conjunction with enhanced sampling based on the metadynamics framework were used. The results show that the solvent choice induces significant differences in the equilibrium ring structures, which may help further resolve the molecular mechanism governing IL-mediated cellulose dissolution.

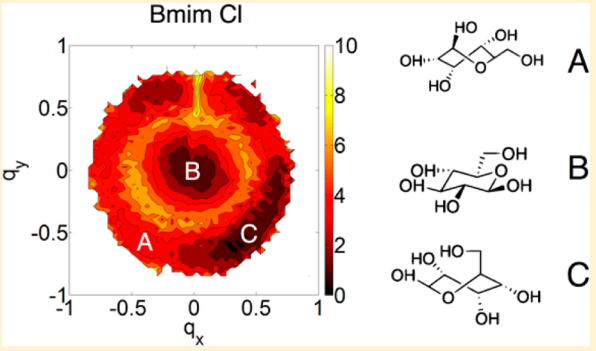

Lignocellulosic biomass is an abundant but underutilized natural resource. Finding efficient methods to efficiently separate biomass into its principle components has been a struggle.[1] A promising route to dissolve recalcitrant biomass is the use of ionic liquids (ILs), some of which have been shown to appreciably dissolve biomass.[2] Through a wealth of experimental and theoretical studies on ILs and biomass, dissolution mechanisms of cellulose have been proposed, giving hope that ILs could supplement or replace current pretreatment methods. The prevailing mechanism supported by computational and experimental research involves disruption of inter- and intracellulose hydrogen bonding by the ionic liquid.[3−10]

One aspect of the interaction between ILs and biomass dissolution that has not been fully explored is the possibility that the IL induces a conformational change within the sugar ring structure. Within crystalline cellulose, the rings are all in the $^4C_1$ conformation, which is expected to be a deep free-energy minimum in both the crystalline and water phases. It is conceivable, therefore, that the disruption of the equilibrium ring structure could be related to the overall thermodynamics governing the dissolution pathway. Probing this effect is challenging to do with either experimentation or classical MD simulations alone. Free-energy calculations coupled with MD simulations are an ideal choice given that the well-known puckering coordinates can serve as coarse-grained descriptors or collective variables (CV) and discriminate between any relevant ring structures. However, as was recently discussed,[11] extreme care should be taken when applying biasing of certain CVs to ring structures.

To study the thermodynamics of the conformational change of a sugar in ionic liquids, we used classical MD simulations[12] (GLYCAM06,[13] GAFF,[14] and TIP3P water[15] and enhanced with the PLUMED[16] plugin) combined with the Parallel Tempering Metadynamics method[17] combined with well-tempered metadynamics.[18] We reduced the number of required replicas by enhancing the potential energy fluctuations through the use of the recently implemented Well-Tempered Ensemble (WTE) approach.[19] The PTMetaD-WTE approach has been applied successfully to protein folding in solution,[20] protein folding on surfaces,[21] and also for observing large scale conformational change in kinase enzymes[22] and is well suited for this task. Glucose was chosen as the model molecule since it is a simple and abundant constituent building block of biomass. On the basis of success of other studies[13,23] in explicit solvent and a vacuum, GLYCAM06 is an ideal choice of force field for explicitly solvated glucose in both water and IL. Three glucose/solvent combinations were considered. A control system of glucose/water was compared to separate simulations of glucose with the ionic liquids 1-butyl-3-methylimidazolium chloride ([Bmim][Cl]) and 1-butyl-3-methylimidazoulim boron tetrafluoride ([Bmim][BF_4]). These two ILs were chosen in order to have a weakly dissolving IL (BF_4) and one that is known to break down crystalline cellulose (Cl). In addition, short unbiased molecular dynamics simulations were used to study the radial distribution functions and solvent structuring. ILs were simulated with the GAFF force field and had point charges scaled by 80%.[24] A detailed description of our procedure is provided in the Supporting Information.

During the metadynamics simulations, we biased the Cremer−Pople spherical puckering coordinates.[25] We biased two metadynamics CVs, the slow puckering coordinates (Φ/θ), and also monitored (without biasing) the fast degree of freedom Q. Using the elegant reweighing scheme proposed by

Received: November 21, 2013
Published: January 14, 2014

Bonomi and co-workers,[26] we then projected the resulting estimate of the free-energy surface (FES) onto the 2D plane (the so-called q_x/q_y plane[27]) of the puckering coordinate space, which is still effective in discriminating between all relevant ring conformers. The need to bias directly the actual spherical CVs and not their Cartesian projections has been previously discussed.[11] Since only the values of the spherical puckering coordinates enter into the definition of the q_x/q_y plane, identification of relevant isomers is not hindered by any potential degeneracy in the $q_z > 0$ vs $q_z < 0$ cases. We note here that the Bonomi et al. reweighting scheme is a necessary step in order to ensure that full sampling of the relevant phase space is achieved. The addition of the parallel tempering aspect of our simulations also ensured full sampling of the phase space accessible by rotation of the exacyclic CH_2OH group. Even with the higher viscosity of the IL systems, the PTMetaD-WTE sampling scheme ensured that all of the relevant states on the q_x/q_y plane were visited and revisited hundreds of times by all of the replicas. Convergence of the free-energy profiles was verified by monitoring the change in free-energy between stable basins on the FES (Figure S1), and the uniqueness of the results was further tested by running a simulation multiple times and comparing the results after a fixed amount of simulation time (Figure S2).

The FESs for glucose in three solvents are shown in Figure 1. While each simulation does have a free-energy minimum

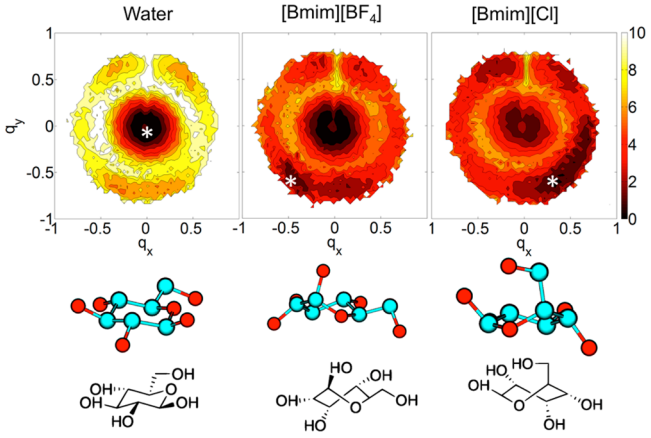

Figure 1. Free energy surfaces of glucose puckering coordinate space in water and two ionic liquids. Asterisks mark the region of the CV space from which the represenative structures that are shown were taken. Conformations left to right: $^4C_1$, $^1S_3$, and ^2S_O. The colorbar is in units of kcal/mol with isolines spaced every 1 kcal/mol.

corresponding to the expected chair conformation ($^4C_1$), there are clear differences between all three solvents. A representative structure from the lowest free-energy basin in each simulation is also shown along with a corresponding 2D line structure for clarity. Interestingly, a simple comparison of the three free-energy profiles immediately suggests some features of the underlying mechanism that lead to preferential dissolution of crystalline cellulose by [Bmim][Cl]. Comparison of the left (water) and middle ([Bmim][BF_4]) FESs shows that, while the relative free-energy scales are changed, the positions of the minima are not. Both simulations have a deep minimum in the chair configuration, with an additional minimum in the $^1S_3$ configuration. We believe it is highly unlikely that a pathway in the q_x/q_y CV space would correspond to a meaningful reaction coordinate, so do not ascribe much meaning to the observed differences in the thermodynamic free-energy barriers between these stable states, although they are somewhat lower in IL. However, it is interesting to see that the relative free energies of these chair and skew configurations are much closer in the [Bmim][BF_4] simulation, while larger differences are observed when comparing [Bmim][Cl] to the other simulations. First, the minimum at the $^1S_3$ configuration is essentially gone and replaced by a much deeper minimum at a different skew conformer ($^2S_0$). Second, the relative free-energy between the center well (chair) and the region favoring the skew is shifted to be around zero, or even slightly favoring the skew. This suggests that significant equilibrium populations of the skew conformer would be present in solution. We also confirmed that the exacyclic CH_2OH group does not play a significant role in any of these thermodynamic preferences. This was done by using the reweighting scheme to calculate the free-energy profiles for the for O−C−C−O linkage connecting the exacyclic group to the ring. The three free-energy profiles were identical within a fraction of 0.25 kcal/mol (both minima and maxima) and displayed the expected characteristic barrier heights one could simply calculate from the respective contribution to the GAFF dihedral force field term. Finally, since the spherical puckering coordinates are thought to be meaningful in identifying catalytic itineraries in enzymatic reactions of sugars,[28] we note that combination of the biased sampling on the spherical puckering coordinates themselves could be combined with existing methods[29] in order to study rates of change between conformers in solution (in addition to the thermodynamic quantities we have described herein).

We further investigated the origin of the thermodynamic driving forces in IL-mediated glucose conformational change by estimating the relative contributions to the observed free-energy differences. We then calculated the free-energy differences between the chair and two skew conformations at each of the temperatures simulated in the PTMetaD-WTE simulation. Using a straight-line fit of these free-energy differences, we then calculated the relative changes in internal energy and entropy using the standard relation $\Delta A = \Delta U - T\Delta S$. The results are shown in Table 1. The change in internal energy and entropy between both skew conformers and the chair conformation in water are similar. In contrast, there are notable differences between the two IL simulations. In general, we observe that change from water to IL results in an entropic increase from the chair to the skew state that is compensated by a much larger energetic decrease. The larger energetic stabilization leads to the aforementioned observations on the free-energy profiles and expected increase in the observed population of other stable ring conformers.

Table 1. The Average and Standard Deviation of Change in Internal Energy and Entropy between the Observed Stable Minima: ^2S_O and $^4C_1$ and $^1S_3$ and $^4C_1$ in kcal/mol and cal/mol/K, Respectively

solvent	water	[Bmim][BF_4]	[Bmim][Cl]
ΔU ($^2S_0 - {}^4C_1$) (kcal/mol)	9.8 ± 0.12	1.7 ± 0.17	−5.3 ± 0.37
ΔS ($^2S_0 - {}^4C_1$) (cal/mol/K)	14.0 ± 0.32	−2.0 ± 1.6	−16.0 ± 0.8
ΔU ($^1S_3 - {}^4C_1$) (kcal/mol)	9.7 ± 0.01	−0.03 ± 0.22	−0.05 ± 0.08
ΔS ($^1S_3 - {}^4C_1$) (cal/mol/K)	13.5 ± 0.1	−6.7 ± 0.7	−5.0 ± 0.3

dx.doi.org/10.1021/ct4010036 | J. Chem. Theory Comput. 2014, 10, 507−510

To study how the conformational changes might be induced by changes in the liquid structure of the IL surrounding the sugar molecule, we performed equilibrium MD simulations and computed the pairwise distribution functions for key distances in the system. As shown in Figure 2, the relative organization

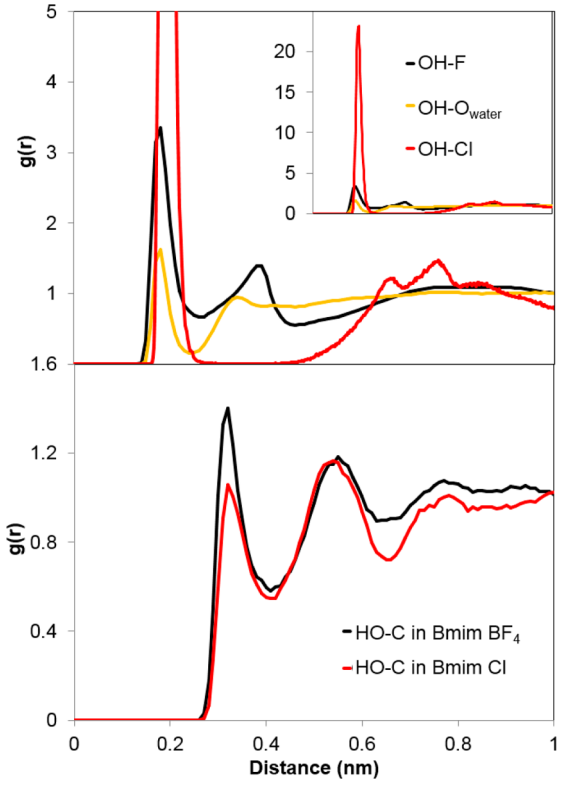

Figure 2. Liquid structure around glucose characterized by radial distribution functions. Top: the association of the hydrogen of glucose's OH groups with oxygen atoms of water, fluorine, or chlorine atoms. Bottom: the association of the C1 carbon (the top of the imidazolium ring in the standard representation) with the oxygen atom of glucose's OH groups.

around the hydroxyl groups of glucose (in the chair conformation) changes significantly between the three solvents. The five radial distribution functions (RDFs) characterize the organization of water and ions around glucose. A similar analysis for glucose and these ILs was also performed by Youngs et al.[30] All liquids show a strong organization of negatively charged ions around the hydrogen atoms of the glucose at about 2 Å. The pair distance corresponding to the first peak heights is similar in all of them because of the similarities in effective atomic size among oxygen, fluorine, and chloride as described by their respective Lennard-Jones parameters. The large peak between Cl and hydroxyl hydrogen atoms is due both to the ability of multiple hydroxyl OH groups to coordinate with a single Cl ion and to the very strong interaction between H and Cl, which leads to the large increase in density at that distance. There is very little discernible anion structure beyond the first well-defined peak due to the layering presence of cations coming close to the glucose molecule after the first solvation shell of anion. As expected, the cation density for the [Bmim][BF_4] system is higher in the first solvation shell compared to the cation in [Bmim][Cl].

The presence of the multiple stable conformations in ILs supports the prevailing mechanism[10,31]—anions disrupt the hydrogen bonding between the chains of a cellulose microfibril by favorable interaction with the hydrogen atoms, which are fundamental to cellulose recalcitrance. The strong correlation between anions and the hydrogen atoms of glucose present in the radial distribution functions supports this hypothesis. Furthermore, the lower local density of oxygen atoms in water than the anions in ILs is further explanation that the attraction between water and cellulose cannot cause dissolution. Therefore, we propose that the strong affinity between hydrogen atoms and anions is the major actor causing dissolution. Considering the free energy barriers are lowered in ILs compared to water, interrupting hydrogen bonds and separating strands of cellulose can be facilitated by the conformational changes of glucan monomers. For example, the anion Cl^- is attracted to the partial positive charge on the hydrogen atoms of cellulose, while the monomers are exploring a wide conformational space. This opens space for the anion to fit between chains of cellulose. The possibility that nearly all conformations can be accessed may be playing a significant role in dissolution.

In this work, we employed a computationally efficient enhanced sampling methodology to study the effects on ionic liquid solvents on the equilibrium structure of cyclic glucose. Previous computational studies of IL-mediated cellulose interactions have focused primarily on the weakened chain−chain interactions that result from strong associations between the sugar monomers and the ionic solvents. Our work suggests that an additional aspect meriting further investigation is whether the individual chains are more easily separated or have different preferred conformational ensembles as a result of the observed differences in ring conformation. Given the wide range of hypothetical IL-based solvents, it is useful to have specific molecular design targets to assist in the rational design of new solvents. An additional future application of the work presented here would be to use computers to screen different types of ILs and extract quantitative structure−property relationships that could be used to specifically define which part of the IL/sugar interaction leads to the observed changes in the equilibrium thermodynamics (i.e., the energetic and entropic driving forces).

■ ASSOCIATED CONTENT

Supporting Information

More information on simulation details and enhanced sampling methods provided. This material is available free of charge via the Internet at http://pubs.acs.org.

■ AUTHOR INFORMATION

Corresponding Author

*E-mail: jpfaendt@uw.edu.

Notes

The authors declare no competing financial interest.

■ ACKNOWLEDGMENTS

The authors acknowledge financial support from NSF grant CBET-1150596 (J.P.) and the Amgen Scholars program (Z.J.). This work was facilitated through the use of computational, storage, and networking infrastructure provided by the Hyak supercomputer system, supported in part by the University of Washington eScience Institute. Mr. Vance Jaeger is thanked for his assistance with computational scripts and algorithms used in preparing this work.

REFERENCES

(1) Tadesse, H.; Luque, R. Advances on Biomass Pretreatment Using Ionic Liquids: An Overview. *Energy Environ. Sci.* **2011**, *4*, 3913−3929.
(2) Maki-Arvela, P.; Anugwom, I.; Virtanen, P.; et al. Dissolution of Lignocellulosic Materials and Its Constituents Using Ionic Liquids‚ÄîA Review. *Ind. Crops Prod.* **2010**, *32*, 175−201.
(3) Cho, H. M.; Gross, A. S.; Chu, J. W. Dissecting Force Interactions in Cellulose Deconstruction Reveals the Required Solvent Versatility for Overcoming Biomass Recalcitrance. *J. Am. Chem. Soc.* **2011**, *133*, 14033−14041.
(4) Gross, A. S.; Bell, A. T.; Chu, J. W. Entropy of Cellulose Dissolution in Water and in the Ionic Liquid 1-Butyl-3-Methylimidazolim Chloride. *Phys. Chem. Chem. Phys.* **2012**, *14*, 8425−30.
(5) Nishiyama, Y.; Sugiyama, J.; Chanzy, H.; Langan, P. Crystal Structure and Hydrogen Bonding System in Cellulose I(Alpha) from Synchrotron X-Ray and Neutron Fiber Diffraction. *J. Am. Chem. Soc.* **2003**, *125*, 14300−6.
(6) Pinkert, A.; Marsh, K. N.; Pang, S. Reflections on the Solubility of Cellulose. *Ind. Eng. Chem. Res.* **2010**, *49*, 11121−11130.
(7) Rabideau, B. A. A.; Ismail, A. Observed Mechanism for the Breakup of Small Bundles of Cellulose I[Alpha] and I[Beta] in Ionic Liquids from Molecular Dynamics Simulations. *J. Phys. Chem. B* **2013**, *117*, 3469−6937.
(8) Zhang, J.; Zhang, H.; Wu, J.; et al. NMR Spectroscopic Studies of Cellobiose Solvation in Emimac Aimed to Understand the Dissolution Mechanism of Cellulose in Ionic Liquids. *Phys. Chem. Chem. Phys.* **2010**, *12*, 1941−7.
(9) Zhao, Y.; Liu, X.; Wang, J.; Zhang, S. Effects of Anionic Structure on the Dissolution of Cellulose in Ionic Liquids Revealed by Molecular Simulation. *Carbohydr. Polym.* **2013**, *94*, 723−730.
(10) Youngs, T. G. A.; Holbrey, J. D.; Mullan, C. L.; et al. Neutron Diffraction, NMR and Molecular Dynamics Study of Glucose Dissolved in the Ionic Liquid 1-Ethyl-3-Methylimidazolium Acetate. *Chem. Sci.* **2011**, *2*, 1594−1605.
(11) Sega, M.; Autieri, E.; Pederiva, F. On the Calculation of Puckering Free Energy Surfaces. *J. Chem. Phys.* **2009**, *130*, 225102.
(12) Hess, B.; Kutzner, C.; van der Spoel, D.; Lindahl, E. Gromacs 4: Algorithms for Highly Efficient, Load-Balanced, and Scalable Molecular Simulation. *J. Chem. Theory Comput.* **2008**, *4*, 435−447.
(13) Kirschner, K. N.; Yongye, A. B.; Tschampel, S. M.; et al. GLYCAM06: A Generalizable Biomolecular Force Field. Carbohydrates. *J. Comput. Chem.* **2008**, *29*, 622−655.
(14) Wu, X.; Liu, Z.; Huang, S.; Wang, W. Molecular Dynamics Simulation of Room-Temperature Ionic Liquid Mixture of [Bmim]-[BF4] and Acetonitrile by a Refined Force Field. *Phys. Chem. Chem. Phys.* **2005**, *7*, 2771−9.
(15) Mahoney, M. W.; Jorgensen, W. L. A Five-Site Model for Liquid Water and the Reproduction of the Density Anomaly by Rigid, Nonpolarizable Potential Functions. *J. Chem. Phys.* **2000**, *112*, 8910−8922.
(16) Bonomi, M.; Branduardi, D.; Bussi, G.; et al. PLUMED: A Portable Plugin for Free-Energy Calculations with Molecular Dynamics. *Comput. Phys. Commun.* **2009**, *180*, 1961−1972.
(17) Bussi, G.; Gervasio, F. L.; Laio, A.; Parrinello, M. Free-Energy Landscape for Beta Hairpin Folding from Combined Parallel Tempering and Metadynamics. *J. Am. Chem. Soc.* **2006**, *128*, 13435−13441.
(18) Barducci, A.; Bussi, G.; Parrinello, M. Well-Tempered Metadynamics: A Smoothly Converging and Tunable Free-Energy Method. *Phys. Rev. Lett.* **2008**, *100*, 020603.
(19) Bonomi, M.; Parrinello, M. Enhanced Sampling in the Well-Tempered Ensemble. *Phys. Rev. Lett.* **2010**, *104*, 190601.
(20) Deighan, M.; Bonomi, M.; Pfaendtner, J. Efficient Simulation of Explicitly Solvated Proteins in the Well-Tempered Ensemble. *J. Chem. Theory Comput.* **2012**, *8*, 2189−21982.
(21) Deighan, M.; Pfaendtner, J. Exhaustively Sampling Peptide Adsorption with Metadynamics. *Langmuir* **2013**, *29*, 7999−8009.
(22) Sutto, L.; Gervasio, F. L. Effects of Oncogenic Mutations on the Conformational Free-Energy Landscape of Egfr Kinase. *Proc. Natl. Acad. Sci. U. S. A.* **2013**, DOI: 10.1073/pnas.1221953110.
(23) DeMarco, M. L.; Woods, R. J. Atomic-Resolution Conformational Analysis of the Gm3 Ganglioside in a Lipid Bilayer and Its Implications for Ganglioside−Protein Recognition at Membrane Surfaces. *Glycobiology* **2009**, *19*, 344−355.
(24) Zhang, Y.; Maginn, E. J. A Simple Aimd Approach to Derive Atomic Charges for Condensed Phase Simulation of Ionic Liquids. *J. Phys. Chem. B* **2012**, *116*, 10036−10048.
(25) Cremer, D.; Pople, J. A. General Definition of Ring Puckering Coordinates. *J. Am. Chem. Soc.* **1975**, *97*, 1354−1358.
(26) Bonomi, M.; Barducci, A.; Parrinello, M. Reconstructing the Equilibrium Boltzmann Distribution from Well-Tempered Metadynamics. *J. Comput. Chem.* **2009**, *30*, 1615−1621.
(27) Biarnés, X.; Ardèvol, A.; Planas, A.; et al. The Conformational Free Energy Landscape of B-D-Glucopyranose. Implications for Substrate Preactivation in B-Glucoside Hydrolases. *J. Am. Chem. Soc.* **2007**, *129*, 10686−10693.
(28) Knott, B. C.; Haddad Momeni, M.; Crowley, M. F.; et al. The Mechanism of Cellulose Hydrolysis by a Two-Step, Retaining Cellobiohydrolase Elucidated by Structural and Transition Path Sampling Studies. *J. Am. Chem. Soc.* **2014**, *136*, 321−329.
(29) Marinelli, F.; Pietrucci, F.; Laio, A.; Piana, S. A Kinetic Model of Trp-Cage Folding from Multiple Biased Molecular Dynamics Simulations. *PLoS Comput. Biol.* **2009**, *5*, e1000452.
(30) Youngs, T. G. A.; Hardacre, C.; Holbrey, J. D. Glucose Solvation by the Ionic Liquid 1,3-Dimethylimidazolium Chloride: a Simulation Study. *J. Phys. Chem. B* **2007**, *111*, 13765−13774.
(31) Lindman, B.; Karlstrom, G.; Stigsson, L. On the Mechanism of Dissolution of Cellulose. *J. Mol. Liq.* **2010**, *156*, 76−81.